J. Applied Membrane Science & Technology, Vol. 28, No. 1, April 2024, 73-90

Chitosan Incorporated with Titanium (IV) Oxide Membrane for Direct Methanol Fuel Cell Application

K. R. Parameswaran[a], N. S. Suhaimin[b], J. Jaafar[a,b]*

[a]School of Chemical and Energy Engineering, Faculty of Engineering, Universiti Teknologi Malaysia, 81310 UTM Johor Bahru, Johor, Malaysia
[b]Advanced Membrane Technology Research Centre (AMTEC), Universiti Teknologi Malaysia, 81310 UTM Johor Bahru, Johor, Malaysia

Submitted: 2/1/2024. Revised edition: 26/3/2024. Accepted: 26/3/2024. Available online: 28/3/2024

ABSTRACT

The direct methanol fuel cell (DMFC), a type of promoted polymer electrolyte membrane fuel cell (PEMFC), has received tremendous attention in the past two decades because of its potential as a promising technology for clean and efficient power generation in the twenty-first century. Over the past four decades, the dominancy of perfluorinated proton exchange membranes (PEM) such as Nafion is prolonging in the current PEM technology due to its chemical stability, high proton conductivity and high mechanical strength in the low operating temperatures. However, the Nafion membrane also has several weaknesses, such as high methanol permeability, high manufacturing cost, and dehydration with low proton conductivity at elevated temperatures > 100°C. This study fabricated a novel composite membrane by blending the pristine chitosan (CS) and titanium oxide (TiO_2) at various loadings, 0.5, 1.0, 1.5 and 2.0 wt% to obtain high performance in DMFC. SEM and FTIR analysis showed that the grafting of (O-Ti-O) successfully incorporated into the CS polymer matrix. Water and methanol uptake of CS/TiO_2 composite membrane decreased with increase of TiO_2 loadings, but proton conductivity value increased. The CS/TiO_2 membrane with 1.5wt.%TiO_2 loading exhibited highest proton conductivity (0.41mScm^{-1}) and lowest methanol permeability (17.18E-08cm^2/s) characteristics among other membranes this due to the hydrophilic TiO_2 raised the membrane hydrophilic character by increasing the number of hydrophilic sites, such as OH-, COO- and O-. The results obtained from the study can be used to conclude that chitosan membrane with TiO_2 filler is a promising high performance PEM candidate for DMFC applications.

***Keywords*:** Chitosan (CS), titanium oxide (TiO_2), polymer electrolyte membrane (PEM), direct methanol fuel cell (DMFC), methanol permeability

1.0 INTRODUCTION

Direct methanol fuel cells (DMFC) are classified as a class of polymer electrolyte membrane fuel cells [1]. They have gained incredible attention due to several advantageous characteristics such as low weight, simplified system design, easy fuel handling, high efficiency, high power density (5.04 $kWhL^{-1}$), and low operating temperature (60ºC-120ºC) [2]. DMFC is regarded as the preferable green energy generation system due to its low emissions. It is utilized for various applications, from transportation to portable applications such as mobile phones, laptops, and computers. DMFC is powered by methanol in liquid form without external reforming and can be operated even at room

* Corresponding to: J. Jaafar (email: juhana@petroleum.utm.my)
DOI: https://doi.org/10.11113/amst.v28n1.288

temperature compared to hydrogen, which operates at temperatures higher than 80ºC [3].

The proton exchange membrane (PEM) is regarded as a fundamental constituent in DMFC, which plays a prominent role as a physical separator and proton conductor, which selectively provide pathways for ion transfer. Over the past four decades, the dominancy of perfluorinated proton exchange membranes such as Nafion is prolonging in the current PEM technology in fuel cells. Nafion membrane has gained massive interest due to its chemical stability, high proton conductivity and high mechanical strength in low operating temperatures. The predominating Nafion membrane is a synthetic perfluorinated ion-exchange polymer with perfluoro ether side chains terminated with sulfonic acid groups randomly distributed along the semicrystalline polymer backbone of (polytetrafluoroethylene). The morphology structure of Nafion, which has an acidic region, plays a vital role in contributing to high proton conductivity at temperatures below 90ºC. Despite the attractive benefits, the practical usage of markedly available Nafion membrane has severe drawbacks for DMFC application, including relatively expensive preparation increasing the overall cost of the fuel cell, environmental inadaptability, complicated synthesis process, dehydration problem with lowering the proton conductivity at high temperature and excessive methanol crossover due to its chemical structure that consequently affected the performance and efficiency of DMFC [4]. The newly developed alternative membrane based on partially fluorinated, acid-base complex, and aliphatic/aromatic hydrocarbon polymers show low production costs over Nafion. However, they suffer from high-temperature dehydration, high methanol crossover, poor proton conductivity and poor durability owing to the attack of hydroxyl (HO) and hydroperoxyl (HOO-) radicals on the native polymeric backbone [5]. Therefore, the massive demand is triggered by developing PEMs with inexpensive, eco-friendly, thermally stable, and durable characteristics, which is a crucial and challenging process. Subsequently, a broad interest has been paid to the biopolymers derived from natural resources owing to their abundance in nature, biocompatibility, and low cost.

As an alternative to the perfluorinated membrane, chitosan (CS) has gained tremendous attention in the world of proton exchange membranes (PEM) for DMFC. CS is derived from the deacetylation of the natural polymer chitin, which can be obtained from shrimp shells [6]. CS as a biopolymer has several advantages, including low methanol permeability, biodegradability, and low cost. Moreover, the solubility of CS in aqueous acetic acid allows it to form a gel, making it an excellent material for membrane synthesis. The presence of the amino ($-NH_2$) and hydroxyl (-OH-) groups in the structure of CS promotes its interaction with other materials/hydrophilic groups, allowing structural alterations to be made to diversify the chemical interactions. The presence of hydroxyl groups in the acetic acid facilitates the dissolution of chitosan via hydrogen bonding with the carboxyl and amine groups from the chitosan.

The chitosan-based inorganic

hybrid membrane is a promising organic-inorganic hybrid to develop a high-performance proton exchange membrane (PEM). The properties of the composite membrane are greatly influenced by the electrostatic force from the interactions between the organic and inorganic particles. It must be highlighted that the proton conductivity of polymer electrolyte membranes heavily relies on the hydrophilicity of the membrane. Tripathi and co-workers successfully developed a composite membrane by blending chitosan organic polymer with inorganic materials such as silica. CS decorated with silica could suppress the movement of methanol and maintain the presence of water in the membrane [7]. Incorporating hydrophilic ceramic oxides such as TiO_2, zirconium oxide, and graphene oxide inside the polymer matrix is a common strategy to enhance the mechanical and thermal stabilities and the proton conductivity with hydrophilic–hydrophobic balance of hybrid membranes. Ceramic filler on the polymer matrix balances its hydrophilic nature, and the chemical activation (doping) of the membranes to produce PEMs with high efficiencies and low costs.

Recently, the development of a chitosan-based inorganic hybrid membrane using modified SiO_2, ZrO_2, and TiO_2 as the inorganic filler is favorable to improve the chitosan membrane performance for DMFC application. The use of ceramic oxides as a filler in biopolymer is attractive due to their environmental and economic importance. Studies have proved that with the introduction of inorganic materials, TiO_2 is a good candidate as a hydrophilic filler for polymer membranes because it helps to maintain suitable hydration of the membrane under fuel cell operating conditions, and the mechanical properties are improved exploitative strategy to improve the proton conductivity of CS-based membrane [8]. The hydrophilic nature of TiO_2 plays a key role in improving the membrane's proton conductivity, which is the most crucial characteristic of a membrane that should have. This is due to the hygroscopic nature of TiO_2 aids the water management within membranes and subsequently improves proton conductivity. Furthermore, these nanocomposite membranes exhibited better electrochemical performance of the cell even at an elevated temperature (110°C) and humidity (30%). The metal–oxide-based inorganic fillers improved the mechanical properties and contributed to the blocking of the fuel, such as methanol, by increasing the transport pathway tortuousness and improving the proton conductivity, which resulted in better cell performance.

Based on the promising characteristics of CS and TiO_2, this study develops, characterizes, and evaluates the overall performance of the flat sheet membrane CS/TiO_2. This novel composite membrane will be fabricated by the solution casting method with the incorporation of various ranges of TiO_2 loading (0.5,1.0,1.5,2.0 wt.%) to obtain the optimum loading value that demonstrates high overall. The composite membrane morphology and interactions analysis is conducted using SEM and FTIR. The physicochemical characterizations by means of water uptake, ion exchange capacity, proton conductivity, and methanol permeability are carried out to determine the overall membrane performance for DMFC applications.

2.0 METHODS

2.1 Materials

Chitosan (CS) ≥ 75% deacetylated, titanium oxide, acetic acid with purity (99.8%), methanol (CH_3OH) (ACS, ISO Reagent) with purity for analysis, potassium hydroxide (KOH) with purity ≥ 99.95% sulfuric acid (H_2SO_4) at 95-97% concentration was supplied by Merck Co, Germany deionized water were used during the experiments.

2.2 Fabrication of Flat Sheet CS/TiO_2 Membrane

To prepare CS/TiO_2 polymeric membrane with 3% (2.25g) chitosan powder dissolved in 0.5M acetic acid (3/4ml of the total solvent volume) in a borosilicate glass. The loadings of TiO_2 varied from 0.5 to 2.0%. The process began with the dispersion of the lowest concentration of the ceramic filler TiO_2 at 0.5% (0.325g) in a separate borosilicate glass with acetic acid (1/4ml of the total solvent volume). Both solutions were stirred simultaneously for an hour at 40°C on a hot magnetic stirrer. Then, CS solution was incorporated with TiO_2 solution, maintaining magnetic stirring at 40°C for 24 hours before the degasification process via sonication. Additionally, sonicate the solution for 30 minutes to produce a homogenous solution. Later, cast the solution on an 8cm x 8cm x 2cm silicone mold and dry it in the oven at a temperature of 40°C for 24 hours. Thenceforth, peel off the formed membrane with an average thickness of 50µm from the silicon mold and then immerse in 2M KOH solution for 24 hours at room temperature. This step is to neutralize the membrane. Finally, the fabricated CS/TiO_2 membrane was washed with deionized water several times until pH 6-7 and dried at the temperature of 37°C. The developed membrane is characterized by its physio-chemical properties.

2.3 Membrane Characterization

The synthesized chitosan modified membranes were characterized to study the physicochemical properties. Scanning Electron Microscopy [9] and Fourier Transform Infrared Spectroscopy (FTIR) were used to analyze each material in an individual membrane.

2.4 Water Uptake

The water uptake of a membrane is defined as the mass ratio of absorbed water to that of the dry membrane. The water intake of the hybrid membrane is calculated by measuring the weight change before and after hydration. The membrane dried in the oven at 60 °C for 48 h to remove the moisture in the membrane. After that, the membrane will be weighted (W_{dry}). The membrane was plunged into deionized water for 24 h at ambient temperature. The swollen membrane (W_{wet}) is weighed as quickly as possible after the surface-attached water of the membrane is drained using filter paper. The water uptake is calculated by using the following equation.

$$\text{Water uptake} = \frac{W_{wet} - W_{dry}}{W_{dry}} \, x \, 100\% \quad (1)$$

2.5 Proton Conductivity

Proton conductivity of the fabricated membrane samples was obtained by electrochemical impedance spectroscopy (EIS) (model of Solartron 1260 Gain phase Analyzer, AMETEK,

Inc., UK) over a frequency range of 1 to 107 Hz with 50 to 500 mV. Initially, all the membranes were fully hydrated by immersing in deionized water for 24 h, and then put onto a home-made two-stainless steel electrode. After that, the measurements of the proton conductivity were calculated using equation 2:

$$\sigma = \frac{L}{RA} \quad (2)$$

where, σ is the membrane conductivity, L is the thickness of the membrane, R is derived from the low intersection of the high frequency semi-circle on a complex impedance plane with the Re(Z) axis and A is the cross-sectional area of membrane.

2.6 Methanol Permeability

Determined the methanol permeability using the diffusion cell method at room temperature. The cell consists of two compartments A and B, separated by the membrane. The membrane equilibrated in distilled water for 24 h. After 24 hours, the thickness of the hydrated membranes was measured three times to obtain the average membrane thickness. Methanol solution was placed on one side of the diffusion compartment (compartment A) with concentration 1 M, and distilled water was placed on the other side (compartment B). A magnetic stirrer was used to agitate in each compartment to ensure the uniformity of solution. Due to concentration differences between the compartments, methanol flow occurs throughout the membrane. The methanol permeability test of all membrane samples was carried out for 3 hours at room temperature and 4ml from sample was taken every half an hour. HPLC-RI was used to provide information to find unknown concentration of the liquid sample. Plotted graph of linear standard curve of methanol concentration versus refractive index to determine the methanol permeability of membranes. Further calculations were made by using the Equation 3.

$$P = a\ x\ \frac{V_B}{A}\ x\ \frac{L}{C_A} \quad (3)$$

where, P is methanol permeability $a = CB\ (t)/\ (t - to)$ the slope of linear interpolation of methanol concentration in the permeate compartment B at time t, $C_B(t)$ versus time, t, V_B is the volume of the water in compartment B, C_A is the methanol concentration in the compartment A at time (t), A is the membrane effective area (cross-sectional area), L is the membrane thickness and t_o is time lag.

2.7 Overall CS/TiO_2 Membrane Characteristics for PEM

Proton conductivity and methanol uptake are essential requirements to enable membranes to be applicable in DMFC. Based on the previous studies, it is known that methanol permeability of CS based membrane decreases to the increasing proton conductivity. Thus, the overall membrane characteristics is the overall performance in terms of the ratio between proton conductivity and the methanol permeability. The membrane with the highest overall characteristics were favored in the DMFC application. The following equation can be assessed to measure the membrane performance:

$$\varphi = \frac{\sigma}{P} \quad (4)$$

Where φ is a parameter that evaluates the overall performance of the membrane in terms of the ratio of the ionic conductivity σ, to the methanol permeability, P.

3.0 RESULTS AND DISCUSSION

Several potential limitations and uncertainty in the experimental approach and data interpretation may arise in this study. The fabrication process of CS/TiO_2 membranes may introduce variability in membrane properties such as thickness, porosity, and composition, which can affect the other parameters such as proton conductivity and methanol permeability measurements, leading to uncertainty in experimental results.

3.1 Surface Morphological Study of CS and CS/TiO_2 Membranes

The synthesized chitosan-modified membranes were characterized to study the physicochemical properties. Scanning Electron Microscopy [9] and Fourier Transform Infrared Spectroscopy (FTIR) were used to analyse each material in an individual membrane.

3.1.1 The Confirmation of the presence of TiO_2 in CS Polymer Matrix

To gather more information about the presence of CS/TiO_2 interconnections, the membranes were characterized by FT-IR, as shown in Figure 1. The ATR-FTIR spectrum presented in Figure 1 shows CS and CS/TiO_2 composite membranes with different loadings of TiO_2. The result showed that the broadening absorption band around 3315cm^{-1} due to the OH bond of chitosan could have an electrostatic interaction of N-H-O-Ti [10]. The band at 3215.18cm^{-1} is the combined peak of the NH_2 and OH stretching vibrations [11]. The band at 3160 cm^{-1} is attributed to the strong interactions between NH_2 and OH with TiO_2 [12]. The band at 2160.51cm^{-1} were allocated to the asymmetrical stretching vibration of the C-H in CH_2 and CH_3 groups [13]. 2100 – 2000 cm^{-1} bands indicate the C-H asymmetric and symmetric vibration due to the TiO_2-OH functional group [14]. 1950-1900 cm^{-1} band is the O-C-NH_2, indicating the presence of the titanates in the composite [15]. 735-1632.85 cm^{-1} bands are associated with the N-H scissoring from the primary amine, and it could be an interaction of Ti^{4+} and -NH_2 [16]. 1541.20-1500 cm^{-1} band formed due to the angular deformations of the N-H bond. Secondary amide, CH_2 bending can be seen at the band 1406.40 cm^{-1}[17]. The peaks in the range from 1400-1385cm^{-1} are attributed to the C-N axial deformation (amine group); C-O stretching from the primary amide [17]. The bands at 1385-1300 cm^{-1} are the C-O-C stretching bands, N=O vibrations, -NH deformations. The band at 1152.68 cm^{-1} is due to the vibrations from the Ti-OH and Ti-O bonds. The 1019.96-895.71cm^{-1} bands have resulted from the C-N bending vibrations and asymmetrical stretching vibrations of C-O glycosidic bonds, Ti-O-C bending mode, and Ti-OH bond. 648.81-599.71cm^{-1} is the Ti-O-Ti bond with the asymmetric stretching mode of Ti-O, immobilization of TiO_2 onto the CS matrix. The band from 580-552.81cm^{-1} is present because of the Ti-O-C. An interaction of the Ti Lewis site with the -NH_2 groups of the CS chain could exist.

3.1.2 Surface Morphology of CS/TiO_2 Membranes

The figures below show that the compactness of the composite membranes is hypothetically increased upon TiO_2 loading up to 2.0 wt.%. The SEM images of surface morphologies of pure CS and CS/TiO_2 nanocomposite films are depicted in Figure 2(a) until Figure 2(e) and cross-section from Figure 2(f) until Figure 2(j). Figure 2(a)

shows pure CS shows a surface structure exceptionally smooth and homogenous surface structure with no obvious defects or cracks (void-free). Figure 2(b) to Figure 2(e) shows that adding nanoparticles to the chitosan matrix developed a topography and granulation on the surface. The appearance of TiO_2 particles in the spherical and distributed uniformly in the film matrix is evidenced in the cross-sectional images of the films. The TiO_2 acts as the filler by filling the empty spaces in the CS polymer matrix. At the lower concentrations (0.5 wt.% and 1.0wt.%), the filler particles appeared scattered in a homogenous pattern and embedded in the matrix. They were well distributed in the chitosan membrane, indicating the immobilization of TiO_2 on the chitosan matrix. The TiO_2 fillers were dispersed homogeneously but with slight difference in particle size within the interspaces of the CS polymer chain and no agglomeration till 1.0wt.%, which may be due to the strong electrostatic interactions between the polymer and nanofillers. It was discovered that increasing the amount of TiO_2 in the CS membrane causes agglomerates of the TiO_2 nanoparticles in the film matrix due to an increase in the number of particles on the chitosan surface and the appearance of a tiny aggregation. Then at a medium higher concentration (1.5wt.%), it was observed that agglomeration of TiO_2 starts to occur in the membrane. The surface of the composite membrane exhibited a certain degree of roughness, accompanied by the nano- TiO_2 particles. Figure 2(e) shows that the nanocomposite film containing 2.0wt% TiO_2 exhibited a larger cluster size of agglomerated TiO_2 nanoparticles than the lower TiO_2 concentrations. The TiO_2 agglomeration is expected to affect the mechanical properties such as proton conduction by blocking effect. Nonetheless, the hydrophilic CS polymer and the TiO_2 fillers proved homogeneous and compatible without any phase separation occurring when a suitable amount of TiO_2 ceramic fillers was added. A similar observation obtained by the author Ubonrat and coworkers, the CS membrane containing TiO_2 fillers that tend to aggregate because of high loading of TiO_2 with an increase in membrane roughness.

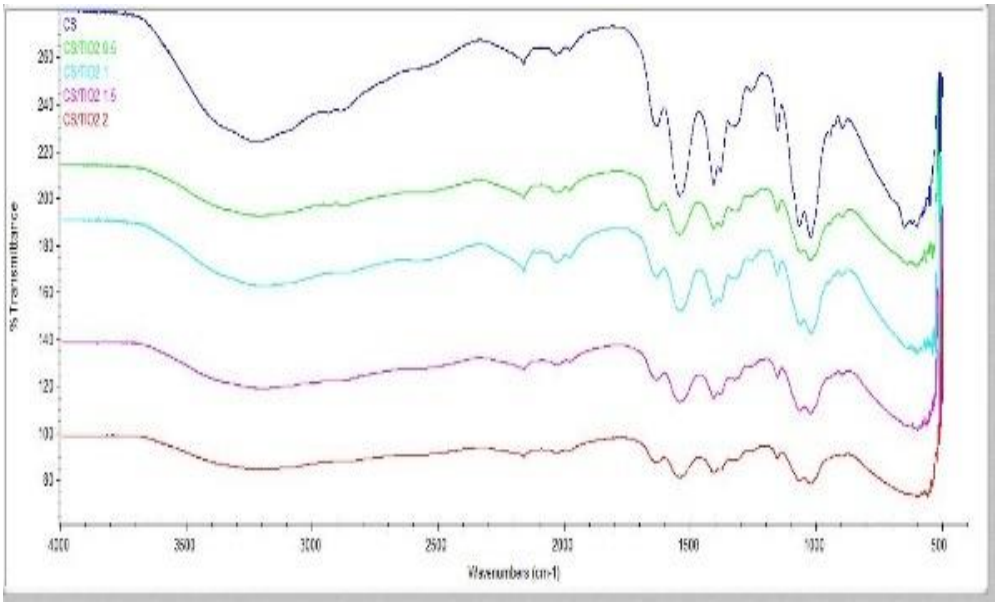

Figure 1 FTIR spectrum of CS and shows CS/TiO_2 composite membrane with different loadings of TiO_2.

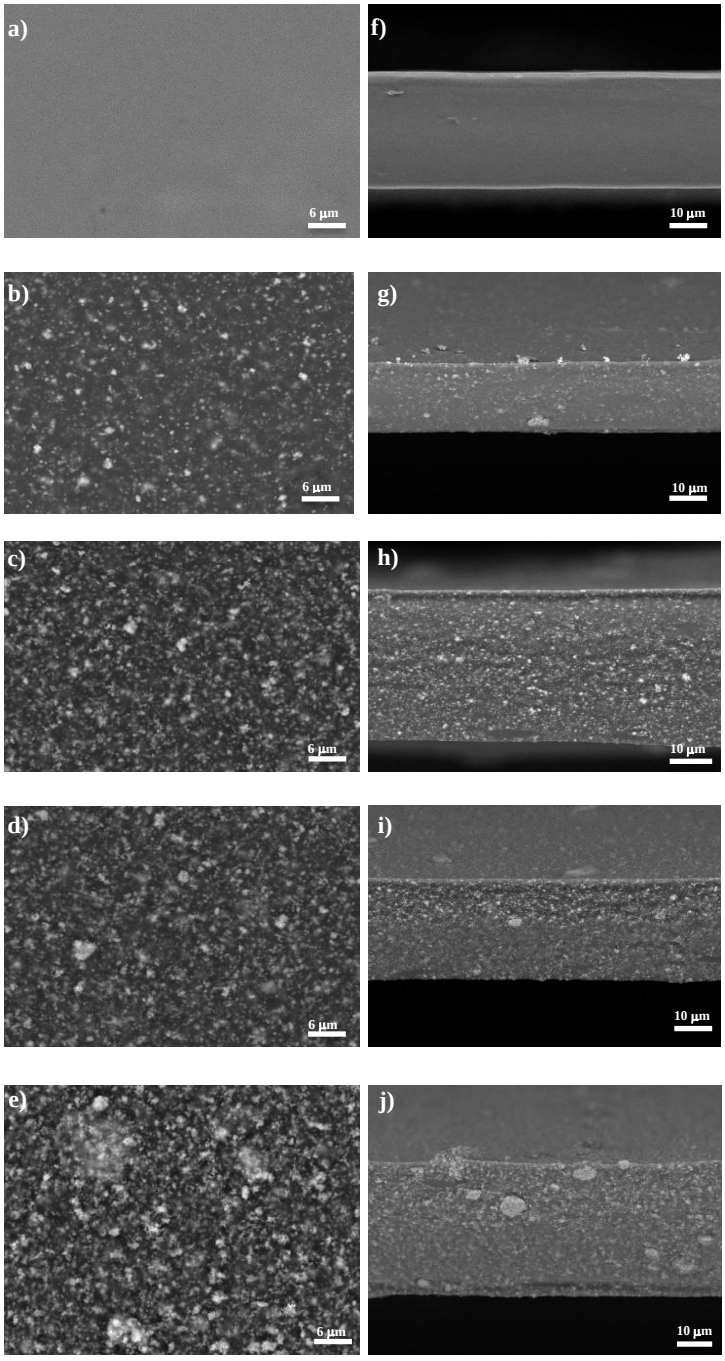

Figure 2 SEM micrographs of surface (a) CS (b) CS/0.5TiO_2 (c) CS/1.0 TiO_2 (d) CS/1.5TiO_2 (e) CS/2.0TiO_2 and cross-section of (f) CS (g) CS/0.5TiO_2 (h) CS/1.0 TiO_2 (i) CS/1.5TiO_2 (j) CS/2.0TiO_2

3.2 Water Uptake of CS/TiO_2 Membrane

Water uptake reflects the capability of a membrane to absorb and hold water, which is desirable for proton conductivity. Water molecules can help vehicle and Grotthuss mechanisms by providing proton carriers and forming hydrogen bond networks, respectively. Water uptake of CS membranes with different TiO_2 loadings at room temperature is presented in Figure 3. The results showed that the CS/TiO_2 composite membranes generally exhibit lower water uptake with increased TiO_2 loadings. Based on the result shown in Table 1, the native CS membrane has the highest overall water uptake at 43.28% compared to other modified membranes. The high-water uptake phenomenon is attributed to the presence of water-soluble polar groups, also known as hydrophilic hydroxyl-OH and amino-NH_2 groups, in the structure of chitosan.

Furthermore, water is orientated inside the polymer matrix by hydrogen bonds or dipoles created by interactions with the polymer's -OH groups and absorbed as free water in the capillary pores [18]. On the other hand, the preliminary introduction of the TiO_2 resulted in a drastic decrease in water uptake from 20.40% to 8.71%. The TiO_2 reduces the crystalline region of chitosan and stiffens the molecules, which reduces the ability to adsorb solvent molecules This study found that the water uptake of the composite membrane exhibits a minor decrease beyond the 0.50wt.% of TiO_2 loadings. This phenomenon is due to the abundant TiO_2 occupying the composite membranes' proton channels, a major water storage zone in the CS matrix; hence water uptake in the composite membranes is reduced [19]. A similar result was obtained from the study [20], which showed that polymer membranes (produced by casting) with high concentrations of TiO_2 or SiO_2 fillers demonstrate a decrease in water absorption. They attribute this phenomenon to the nature of these fillers. When incorporating the nanoparticles in the polymeric membrane at the lowest concentration, a behaviour similar to that of the unfilled membrane is obtained due to the minimal competition between the dispersed particles and the water in the porous spaces.

Meanwhile, for the CS/1.5TiO_2, the percentage of water uptake shows a sudden increment. This can occur when an adequate dispersion of the ceramic filler particles can cause some defects or vacancies in the matrix, thus generating a free volume at the interface between these ceramic particles and the polymer chain where the absorption capacity and retention of water molecules of the polymeric compound are improved. Moreover, the excessive loading of TiO_2 can be correlated to the morphological structure of the CS/TiO_2 that seems to exhibit severe agglomeration of TiO_2 and reduces the water absorption capacity by restricting the CS polymeric matrix channels. When the TiO_2 content was higher than 2.0wt.%, the total amount of hydroxyl groups on the surface of TiO_2 particles decreased due to the aggregation of TiO_2 particles. The obtained SEM micrographs can support this statement. Therefore, the hydrophilicity of CS/TiO_2 hybrid membranes decreased, leading to decreased water uptake. In addition, due to the dilution effect of the polar groups of the polymers and to the interference of the ceramic particles in the porous spaces commonly occupied by water, resulting in a smaller volume of effective water absorption.

Table 1 Water uptake of the membranes with different loadings of TiO_2

Membrane type	Thickness (mm)	Average weight, before (g)	Average weight, after (g)	Water uptake (%)
CS	0.0051	0.27	0.27	1.74
CS/0.5TiO_2	0.0055	0.35	0. 36	0.82
CS/1.0TiO_2	0.0054	0.45	0.45	0.38
CS/1.5TiO_2	0.0053	0.17	0.17	1.29
CS/2.0TiO_2	0.0054	0.3	0.30	0.20

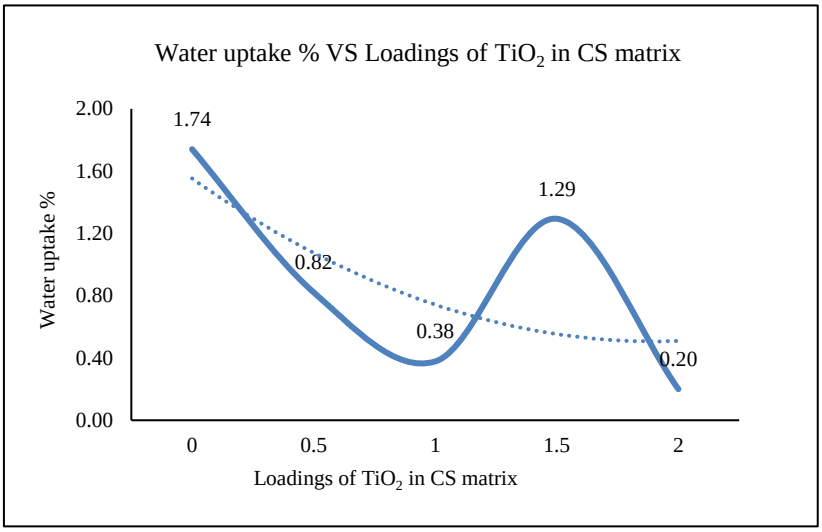

Figure 3 Graph of water uptake (%) of CS/TiO_2 with different weight ratio of TiO_2

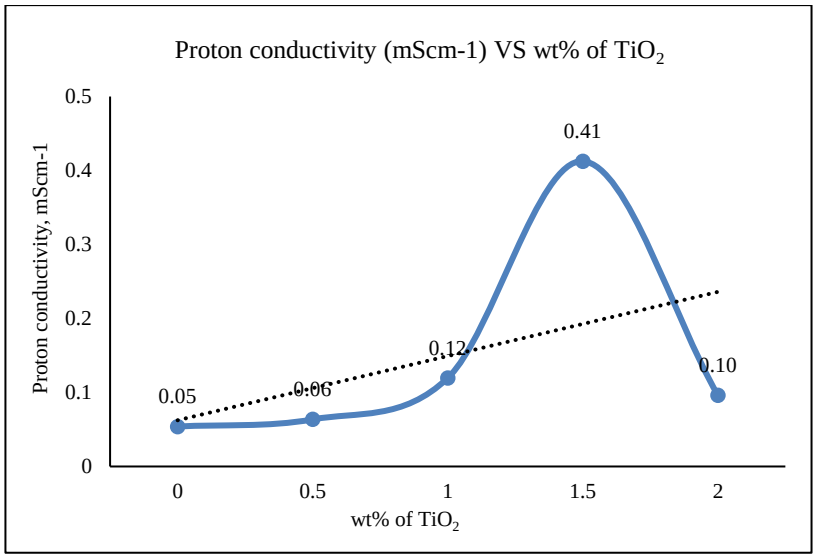

Figure 4 Graph of Proton conductivity ($mScm^{-1}$) of pristine and composite membranes versus wt% of TiO_2

3.3 Proton Conductivity of CS/TiO_2 Membranes

Many studies have reported that composite membranes exhibit higher conductivity than their native membranes. In general, inorganic fillers improve the creation of proton transport channels inside the membrane, increase the water retention capacity, add conductive groups, and improve conductivity. In this study, the membranes display an increasing proton conductivity trend as the wt% of TiO_2 increases in the membrane (refer Figure 4 and Table 2). This increase in proton conductivity is due to the moisture absorption capacity in each composite membrane (CS/TiO_2) controlled by the incorporation of the inorganic ceramic filler (TiO_2). The ionic conductivity increases with the introduction of ceramic oxide materials in the polymer matrix [21]. The water uptake of the modified CS membrane with TiO_2 was lower than the native CS membrane. This phenomenon can be elucidated by the presence of free water and bound water retained in the current membrane. The hygroscopic nature of TiO_2 particles occupied the nanopores of the hydrophilic CS membrane without contending with water molecules. Thus, water contact ionization produces the electric charge from the oxide particles. In contact with that, the hydroxyl groups are formed in a monolayer on the surface of TiO_2.

Hence, TiO_2 release water whenever the membrane needs water without external humidification for superior proton conductivity. Hydrophilic domains are thought to act as a proton pathway, increasing proton conductivity [22]. Furthermore, adding hydrophilic inorganic fillers raised the membrane's hydrophilic character [23] by increasing the number of hydrophilic sites, such as OH^-, COO^- and O^- [24]. As the TiO_2 particle size is sufficiently small, the existing waters of hydration of sulfuric acid may form a bridge between shrunken clusters, thereby providing a pathway for proton hopping from one cluster to another [25]. For instance, CS/0.5TiO_2 and CS/1.0TiO_2 exhibited a lower water uptake than pristine CS. However, the proton conductivity of the membrane, which consists of 0.5wt% and 1.0wt% of TiO_2, shows a slight increment in the proton conductivity compared to the pristine membrane. This may be due to the homogenous dispersion of TiO_2 to the CS matrix creating plenty of available volumes in polymer and several ion-exchangeable sites per cluster, allowing for easier water molecule penetration through the membrane and, consequently, providing continuous proton conducting channels for fast proton migration. Therefore, the mobility of hydrogen ions improved with the increase. The obtained SEM micrograph can support the homogenous dispersion of TiO_2 in the CS matrix surface. Conversely, the water uptake of CS/1.5TiO_2 is higher than CS/2.0TiO_2. Higher water uptake contributes substantially to the formation of hydrophilic properties in membranes capable of facilitating proton transport even under low humidity conditions. The low proton conductivity in CS/2.0TiO_2 due to the structure of this membrane possesses a compact network that makes it difficult for water to pass through [26].

Moreover, when the content of the TiO_2 was too high, severe aggregation of the fillers resulted in to decrease in the effective surface area of the particles, leading to the decrease of the water uptake as shown in Figure 3 hence blocking the proton conducting pathway resulting in low proton conductivity. Incorporation of TiO_2 particles into CS, though all membranes have small water uptake under low relative humidity, they still show a great

increase in proton conductivity compared to the pristine CS membrane. The addition of TiO_2 has also formed a much denser and closer distribution of TiO_2 clusters in the CS membrane matrix. It was well understood that the hygroscopic nature of TiO_2 has successfully contributed to enhancing the single-cell performance by generating a higher proton conductivity, as shown in Figure 4.

3.4 Methanol Permeability

Methanol permeability is the product of the diffusion coefficient and sorption coefficient. The diffusion coefficient reflects the effect of a surrounding environment on the molecular motion of the permeant, and the sorption coefficient correlates with the concentration of a component in the fluid phase. Another key feature of a good electrolyte for electrochemical applications is the ability to separate the anode and cathode sides [25]. An electrolyte must prohibit reactants from crossing from the anode to the cathode or vice versa. Because of the crossover problem, direct reactivity between the reactants reduces electron production, hence lowering the current and voltage of the electrochemical device provided. Due to high solubility in water, the electro-osmotic drags in the PEM causes the methanol molecules to cross paths with water molecules during the DMFC operation. As a result, an effective PEM membrane for DMFC the membrane must be able to prevent methanol from crossing to the cathode side. The ability of a PEM membrane to withstand methanol migration through its structure was measured using methanol permeability. Figure 5 illustrates the methanol permeation of native and composite membranes as a function of time (s). Based on the result, the methanol permeability of the polymer membrane of the CS matrix (4.66 x 10-7) is lower compared to Nafion 117 membrane (25×10^{-7}) (refer Table 2). The lower methanol crossover is likely due to the differences in microstructure between CS and Nafion.

Meanwhile, the methanol permeability of the TiO_2-doped membrane is much lower than the undoped membrane. This phenomenon may be due to TiO_2 contributes to increase the tightness of the composite membrane, thus it can suppress little methanol and diffuses into the membrane composite [27]. Therefore, as the TiO_2 content increases the diffusion capacity of nanocomposite membranes for methanol is suppressed as well. This owing to the availability of TiO_2 can improve the interaction with chitosan matrix via hydrogen bonds. Given the strong interaction, the membrane structure more dense, thus restricting the movement of methanol into the membrane which called as “blocking effect”. In addition, the methanol uptake of PEMs depends greatly on the available space within membranes and also study from [28] stated that the high aspect ratio with higher surface area of adequate filler loading can provide a tortuous pathway for methanol crossover and eventually can hinder the methanol permeation. Thenceforth, the aggregation of the TiO_2 fillers results in a decrease in the effective surface area of the particles, leading to the decrease of the methanol.

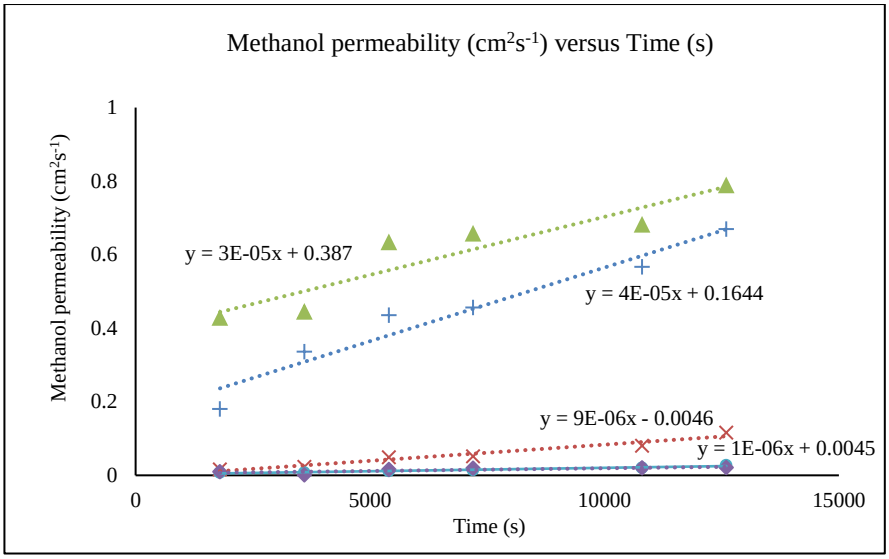

Figure 5 Graph of methanol permeability (cm^2s^{-1}) versus Time(s)

Table 2 Overall performance of native and composite membranes

Membrane type	**Proton conductivity $mScm^{-1}$**	**Methanol permeability cm^2/S**	**Overall membrane characteristic φ**
CS	0.05	4.61E-07	11583.03
CS/0.5TiO_2	0.06	3.76E-07	17305.02
CS/1.0TiO_2	0.12	1.28E-07	553987.87
CS/1.5TiO_2	0.41	1.18E-08	2401028.85
CS/2.0TiO_2	0.10	1.22E-08	94090.43

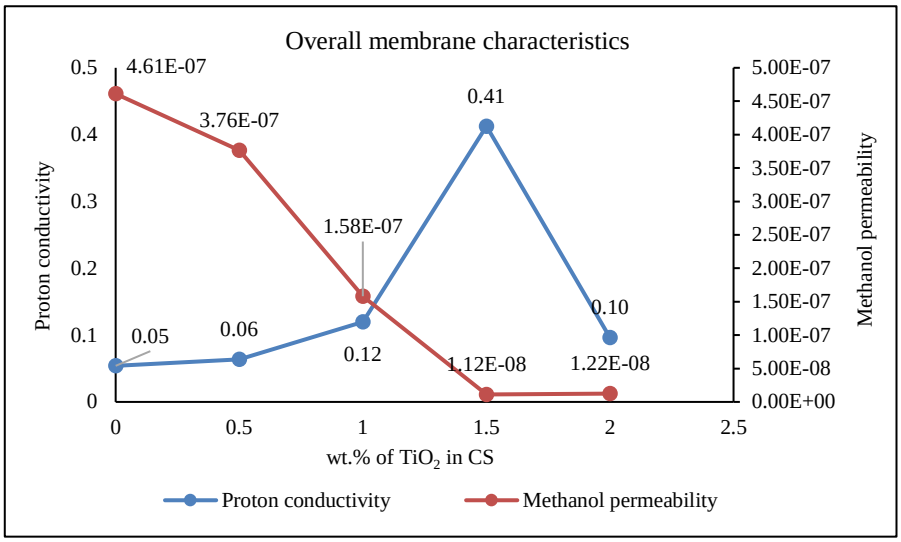

Figure 6 Graph of overall membrane characteristics

Table 3 Comparison between study data and literature review data

Membrane type	Proton conductivity mScm^{-1}	Methanol permeability cm^2/S	Reference
CS	0.054	4.61E-07	
CS/0.5TiO_2	0.063	3.76E-07	
CS/1.0TiO_2	0.12	1.28E-07	
CS/1.5TiO_2	0.41	1.18E-08	
CS/2.0TiO_2	0.096	1.22E-08	
CS/STiO_2	0.0122	3.3 × 10-7	[29]
PVA/TiO_2/ Nafion®	0.0901	8.4 ×10-7	[30]
F–TiO2– NT/Nafion®	0.092	8.6 ×10-8	[5]
Ru85Se15/ TiO_2/C	0.029	3.77 × 10-7	[31]
PVA/nt– TiO_2/ PSSA	0.1197	2.08 ×10-6	[32]

3.5 Comparison between Study Data and Literature Review Data

The results from the study show improvements in both proton conductivity and methanol permeability compared to the membranes reported in the literature review (refer Table 3). The CS/1.5TiO_2 membrane in this study particularly stands out with significantly enhanced proton conductivity and remarkably low methanol permeability, making it a promising candidate for direct methanol

fuel cell (DMFC) applications (refer Figure 6).

Proton conductivity indicates the ability of the electrolyte membrane to transport protons (H^+) from the anode to the cathode. High proton conductivity is crucial for effective ion transport, which directly affects the efficiency of the electrochemical reactions at the electrodes.

For efficient DMFC operation, the membrane should have high proton conductivity to facilitate rapid proton transportation, which enabling fast electrochemical reactions and thus high power output. With the high proton conductivity measured in this study, it indicates that CS/1.5TiO_2 can efficiently transport protons, which able to generate high power output.

Methanol permeability refers to the rate at which methanol molecules can pass through the membrane in the DMFC system. High methanol permeability can lead to methanol crossover from the anode to the cathode, reducing the cell's efficiency and causing fuel wastage. Ideally, the membrane should have low methanol permeability to minimize methanol crossover and maximize the utilization of methanol at the anode. Therefore, with the lowest methanol permeability measured in CS/1.5TiO_2 membrane, it indicates this membrane could offer a better performance in the DMFC operation, as it effectively obstruct the methanol crossover and improve fuel efficiency.

Overall, the addition of TiO_2 nanoparticles to chitosan membranes appears to be a successful strategy for enhancing their performance in DMFC applications. The results from the study suggests that the incorporation of TiO_2 nanoparticles into chitosan membranes enhances their performance in DMFC applications by simultaneously improving proton conductivity and reducing methanol permeability. This indicates the potential of TiO_2-based chitosan membranes as efficient proton exchange membranes for clean and efficient power generation in DMFCs.

4.0 CONCLUSION

CS/TiO_2 membranes were successfully fabricated by the solution casting method, whereby chitosan with 1.5wt.% of TiO_2 membrane exhibits exceptional performance, high proton conductivity and low methanol permeability. This superior combination of properties is attributed to the synergistic effects of chitosan and TiO_2 nanoparticles, which enhance proton transport while effectively mitigating methanol crossover. In addition, the successful integration of 1.5 wt% of TiO_2 nanoparticles into the chitosan matrix yielded a well-dispersed morphology of PEM. Hence, further efforts should be performed with aiming to optimize the PEM fabrication process and scaling up production, pertaining to pave the way for the practical implementation of CS/1.5TiO_2 membranes in real-world DMFC systems, contributing to the advancement of clean and efficient power generation technologies.

CONFLICTS OF INTEREST

The authors declare that there is no conflict of interest regarding the publication of this paper.

ACKNOWLEDGEMENT

We are grateful to AMTEC and the School of Chemical and Energy Engineering for the facilities provided that contribute to the success of this study. We also would like to acknowledge the Research

Management Center (RMC), UTM for the financial funding through the UTM-TDR research grant.

REFERENCES

[1] Mohanapriya, S. and V. Raj, (2018). Cesium-substituted mesoporous phosphotungstic acid embedded chitosan hybrid polymer membrane for direct methanol fuel cells. *Ionics*, *24*(9), 2729-2743.

[2] Junoh, H., *et al.* (2020). Synthetic polymer-based membranes for direct methanol fuel cell (DMFC) applications. *Synthetic Polymeric Membranes for Advanced Water Treatment, Gas Separation, and Energy Sustainability*, 337-363.

[3] Othman, M. H., A. Ismail, and A. B. Mustafa. (2010). Recent development of polymer electrolyte membranes for direct methanol fuel cell application – A review. *Malaysian Polym. J.*

[4] Suhamin, N. S., *et al.* (2021). Nanocomposite membrane by incorporating graphene oxide in sulfonated polyether ether ketone for direct methanol fuel cell. *Materials Today: Proceedings*, *46*(5), 2084-2091.

[5] Ranjani, M., *et al.* (2019). Chitosan/sulfonated graphene oxide/silica nanocomposite membranes for direct methanol fuel cells. *Solid State Ionics*, *338*, 153-160.

[6] Muhmed, S. A., *et al.* (2019). Emerging chitosan and cellulose green materials for ion exchange membrane fuel cell: A review. Energy. *Ecology and Environment*, *5*(2), 85-107.

[7] Tripathi, B. P. and V. K. Shahi. (2011). Organic–inorganic nanocomposite polymer electrolyte membranes for fuel cell applications. *Progress in Polymer Science*, *36*(7), 945-979.

[8] Yang, D., *et al*. (2009). Chitosan/TiO_2 nanocomposite pervaporation membranes for ethanol dehydration. *Chemical Engineering Science*, *64*(13), 3130-3137.

[9] Shakeri, S. E., *et al*. (2013). Polyelectrolyte nanocomposite membranes, based on chitosan-phosphotungstic acid complex and montmorillonite for fuel cells applications. *Journal of Macromolecular Science, Part B, 52*(9), 1226-1241.

[10] Díaz-Visurraga, J., *et al*. (2010). Semitransparent chitosan-TiO_2 nanotubes composite film for food package applications. *Journal of Applied Polymer Science,* 116.

[11] Alagumuthu, G. and T. A. Kumar. (2013). Synthesis and characterization of chitosan/TiO_2 nanocomposites using liquid phase deposition technique.

[12] Tatarinov, D. A., S. R. Sokolnikova, and N. A. Myslitskaya. (2021). Applying Chitosan- TiO_2 nanocomposites for photocatalytic degradation of anthracene and pyrene, *7*(1).

[13] Huang, K.-S., *et al.* (2014). Imobilization and stabilization of TiO_2 nanoparticles in alkaline-solidificated chitosan spheres without cross-linking agent.

[14] Zainal, Z., *et al*. (2009). Characterization of TiO (2)-chitosan/glass photocatalyst for the removal of a monoazo dye via photodegradation-adsorption process. *J Hazard Mater*, *164*(1), 138-45.

[15] Habiba, U., *et al*. (2016). Adsorption and photocatalytic degradation of anionic dyes on chitosan/PVA/Na-Titanate/TiO_2 composites synthesized by

solution casting method. *Carbohydr Polym.*, *149*, 317-31.

[16] Zhang, L., *et al.* (2015). Synthesis of titanium cross-linked chitosan composite for efficient adsorption and detoxification of hexavalent chromium from water. *Journal of Materials Chemistry A*, *3*(1), 331-340.

[17] Nithya, A., and K. Jothivenkatachalam. (2014). Visible light assisted TiO_2-chitosan composite for removal of reactive dye. *J. Environ. Nanotechnol.*, *3*(3), 20-26

[18] Ruiz Gómez, E. E., J. H. Mina Hernández, and J. E. Diosa Astaiza. (2020). Development of a Chitosan/PVA/TiO_2 nanocomposite for application as a solid polymeric electrolyte in fuel cells. *Polymers*, *12*(8).

[19] Zhang, H., *et al.* (2013). Enhanced proton conductivity of sulfonated poly (ether ketone) membrane embedded by dopamine-modified nanotubes for proton exchange membrane fuel cell. *Fuel Cells*, *13*(6), 1155-1165.

[20] Yang, C.-C., W.-C. Chien, and J. li. (2010). Direct methanol fuel cell based on poly (vinyl alcohol)/titanium oxide nanotubes/poly (styrene sulfonic acid) (PVA/nt-TiO_2/PSSA) composite polymer membrane. *Journal of Power Sources*, *195*, 3407-3415.

[21] Ramírez-Salgado, J. (2007). Study of basic biopolymer as proton membrane for fuel cell systems. *Electrochimica Acta*, *52*(11), 3766-3778.

[22] Onuma, A., *et al*. (2015). Effect of the addition of hydrated titanium oxide on proton conductivity for aromatic polymer electrolyte membrane. *Solid State Ionics*, 277.

[23] Gnus, M., G. Dudek, and R. Turczyn. (2018). The influence of filler type on the separation properties of mixed-matrix membranes. *Chemical Papers*, *72*(5), 1095-1105.

[24] Junoh, H., *et al.* (2020). Performance of polymer electrolyte membrane for direct methanol fuel cell application: perspective on morphological structure. *Membranes (Basel)*, 10(3).

[25] Karim, M. A. (2021). Titanium dioxide nanoparticle incorporated PVDF-HFP based composite membrane for direct methanol fuel cells application. Bangladesh *Journal of Scientific and Industrial Research*, *56*, 125-132.

[26] Yang, T., *et al.* (2018). A graphene oxide polymer brush based cross-linked nanocomposite proton exchange membrane for direct methanol fuel cells. *RSC Advances*, *8*(28), 15740-15753.

[27] Bauer, F., and M. Willert-Porada. 2005. Characterisation of zirconium and titanium phosphates and direct methanol fuel cell (DMFC) performance of functionally graded Nafion (R) composite membranes. *Journal of Power Sources*, *145*, 101-107.

[28] Ismail, A., *et al*. (2012). Modification of Sulfonated Poly (Ether Ketone) for DMFC Application. In book: Membrane Modification. 409-448.

[29] Gandhi, K., B. K. Dixit, and D. K. Dixit. (2012). Effect of addition of zirconium tungstate, lead tungstate and titanium dioxide on the proton conductivity of porous polystyrene membrane. *International Journal of Hydrogen Energy*, *37*(4), 3922-3930.

[30] Gouda, M., T. Tamer, and M.

Mohy Eldin. (2021). A highly selective novel green cation exchange membrane doped with ceramic nanotubes material for direct methanol fuel cells. *Energies, 14*, 5664.

[31] Cui, Z., *et al.* (2009). Chitosan/heteropolyacid composite membranes for direct methanol fuel cell. *Journal of Power Sources, 188*(1), 24-29.

[32] Vijayalekshmi.V and D. Khastgir. (2018). Fabrication and comprehensive investigation of physicochemical and electrochemical properties of chitosan-silica supported silicotungstic acid fuel cell applications. *Energy, 142*, 313-330.

[33] Ahmed, S., *et al*. (2021). Preparation and characterization of a novel sulfonated titanium oxide incorporated chitosan nanocomposite membranes for fuel cell application. membranes, *Membranes, 11*(6), 450.

[34] Palani, P. B., *et al.* (2014). Improvement of proton conductivity in nanocomposite polyvinyl alcohol (PVA)/chitosan (CS) blend membranes. *RSC Advances*, *4*(106), 61781-61789.